Available online at www.sciencedirect.com
SCIENCE DIRECT
Journal of Catalysis 242 (2006) 26–37
JOURNAL OF CATALYSIS
www.elsevier.com/locate/jcat

Alkyne hydrogenation over Pd catalysts: A new paradigm

Detre Teschner [a,b,*], Elaine Vass [a], Michael Hävecker [a], Spiros Zafeiratos [a], Péter Schnörch [a], Hermann Sauer [a], Axel Knop-Gericke [a], Robert Schlögl [a], Mounir Chamam [b], Attila Wootsch [b], Arran S. Canning [c], Jonathan J. Gamman [c], S. David Jackson [c], James McGregor [d], Lynn F. Gladden [d]

[a] *Fritz-Haber-Institut der MPG, Faradayweg 4-6, D-14195 Berlin, Germany*
[b] *Institute of Isotopes, Hungarian Academy of Sciences, P.O. Box 77, Budapest H-1525, Hungary*
[c] *WestCHEM, Department of Chemistry, University of Glasgow, Glasgow G12 8QQ, Scotland, UK*
[d] *University of Cambridge, Department of Chemical Engineering, New Museums Site, Pembroke Street, Cambridge CB2 3RA, UK*

Received 12 April 2006; revised 29 May 2006; accepted 31 May 2006

Available online 30 June 2006

Abstract

The hydrogenation of 1-pentyne over various palladium catalysts was studied under various conditions. In the regime of selective hydrogenation, as observed by in situ X-ray photoelectron spectroscopy, significant amounts of subsurface carbon and a Pd-C surface phase built up in the early stage of the reaction. These species inhibited the emergence of bulk-dissolved hydrogen to the surface, which is reactive but unselective. Carbon laydown was also observed by tapered element oscillating microbalance and by catalytic pulse experiments, with greater laydown occurring in the selective regime. The effect of carbon dissolution in the crystal lattice near the surface was evidenced by high-resolution transmission electron microscopy. In alkyne hydrogenation, the active phase of palladium catalysts is a Pd-C surface phase in the regime of selective hydrogenation. Because self-hydrogenation (hydrogen from dissociated pentyne) was also shown to be unselective, only surface hydrogen from the gas phase is available to generate the alkene. The issue of structure-sensitivity of alkyne hydrogenation over palladium catalysts is discussed in terms of structure-sensitive carbon deposition and carbon dissolution into the metal lattice.

Keywords: Palladium; 1-Pentyne; Selective hydrogenation; Carbon deposition; High-pressure XPS; TEOM; HRTEM

1. Introduction

Palladium is one of the most important hydrogenation catalysts used in industry and studied in fundamental research. Its uses include the removal of acetylene from ethylene feedstocks [1]. While in contact with the reactant feed, the catalyst can undergo different transformations, including β-hydride formation, carbon deposition, green oil formation, or carbon dissolution in the metal. Therefore, it is not surprising that various explanations have been offered to explain palladium's ability to selectively hydrogenate multiple unsaturated hydrocarbons [2–9]. Most of the models consider the presence of a carbonaceous overlayer. In the hydrogenation of C_2H_2, Webb et al. [2,3] proposed that the reaction proceeds in the second layer, on top of an irreversibly adsorbed first layer. In this way, the hydrocarbonaceous deposit was thought to be the carrier of activity, via hydrogen transfer from the first layer to the second layer. Ponec et al. [4,5] suggested that the deposited carbon was only a selectivity modifier through site isolation. This idea was put forward by others [6–8,10] envisaging catalytic sites of different sizes between carbon deposits. These can lead to different adsorption geometries and/or owing to steric hindrance of the reactant to different reaction products. The effect of carbonaceous deposits on skeletal hydrocarbon transformation was thoroughly studied by Paál and co-workers [11,12]. Elsewhere, a carboneceous overlayer on Pd(111) was shown to shift the methanol oxidation selectivity toward formaldehyde formation [13].

There is significantly less information in the literature about gas-phase hydrogenation involving longer-chain alkynes. In the

* Corresponding author. Fax: +49 30 8413 4676.
E-mail address: teschner@fhi-berlin.mpg.de (D. Teschner).

0021-9517/$ – see front matter
doi:10.1016/j.jcat.2006.05.030

selective hydrogenation of propyne to propene, an early non-steady-state regime was observed associated with significant carbon laydown [14]. Kennedy et al. [15] attributed the active site for propene formation to a hydrocarbonaceous overlayer, formed during the early stages of the reaction sequence. It was shown that propene was produced only after a significant amount of carbon was retained on the catalyst. Transient catalytic and in situ IR spectroscopic studies indicated a similar situation in butyne hydrogenation [16–18]. Furthermore, the survey of the literature indicates some sort of structure sensitivity of palladium catalysts in alkyne hydrogenation [15,17,19,20], which is in strong contrast to the accepted structure insensitivity of hydrogenation.

Using X-ray diffraction (XRD), formation of PdC_x solution was observed when contacting Pd Black with acetylene [21]. Approximately 3% lattice expansion was calculated for 15% incorporated carbon ($PdC_{0.15}$). Several other studies confirmed the dissolution of carbon in the palladium bulk [22–24]. Recent density functional theory (DFT) calculations [25] revealed that carbon insertion into the Pd surface is an energetically favorable process and that the most stable sites are located between the first and second surface layers, that is, in the subsurface position. This latter was also observed experimentally by scanning tunneling microscopy (STM) [26].

Although the golden era of studying the mechanism of hydrogenation processes has long since passed, the current status of mechanistic information cries out for an in situ investigation throughout the course of reaction with the ability to (i) look at the surface selectively from the bulk, (ii) quantify the amount of carbon deposition, and (iii) perform a depth-profiling experiment. Our novel high-pressure X-ray photoelectron spectroscopy (XPS) system operated at a synchrotron source offers all of these capabilities. The XPS measurements were complemented by various reaction studies, by high-resolution transmission electron microscopy (HRTEM), and by in situ tapered element oscillating microbalance (TEOM) experiments. The latter allowed us to quantify the amount of adsorbed molecules during hydrogenation and also the amount of retained carbon. The experimental approach that we followed was to demonstrate on a typical Pd/Al_2O_3 catalyst the phenomenologic descriptions of alkyne hydrogenation while other better-suited samples were applied in spectroscopy and TEM. However, to justify the generality of observation, care was always taken to produce as much overlap as possible in the "matrix of examined materials and experimental methods." For example, in situ XPS and TEOM experiments were carried out on both bulk Pd samples and supported catalysts. Here we present experimental evidence that the selective hydrogenation of C≡C triple bond proceeds not on metallic palladium, but rather on a "PdC surface phase" formed during the reaction.

2. Experimental

2.1. Catalytic hydrogenation

Pulse hydrogenation of 1-pentyne was performed in a pulse-flow microreactor system. The catalyst (0.1 g, 200 μm, 1% $Pd/\theta\text{-}Al_2O_3$, ex-Johnson–Matthey, 31.1% dispersion) was reduced in situ in flowing hydrogen (25 $cm^3\,min^{-1}$) at 6 bar and 313 K for 30 min. The flow was then switched to helium (25 $cm^3\,min^{-1}$) and aliquots of 1-pentyne (10 μl) pulsed over the catalyst at 303 K. This methodology ensured that the palladium surface was saturated with hydrogen. Pulses were also passed over a catalyst that had been heated to 473 K in flowing helium after reduction. This temperature is above the hydrogen desorption temperature from palladium [27]; hence this methodology ensured that no hydrogen was retained by the palladium surface. The gases evolved were analyzed by a gas chromatograph fitted with a flame ionization detector (FID) and a CP Al_2O_3/Na_2SO_4 column; C-to-Pd ratios were calculated from the gas chromatography (GC) trace according to mass balance.

A continuous-flow microreactor system was used for vapor-phase hydrogenation of 1-pentyne. The 1% $Pd/\theta\text{-}Al_2O_3$ catalyst (0.1 g) was reduced in situ in flowing hydrogen. 1-Pentyne was introduced into the hydrogen feedstream via a saturator held at 273 K. The 1-pentyne:hydrogen ratio was 1:4 at a flow rate of 25 $cm^3\,min^{-1}$. The reaction was performed at 308 K. After 2 h on stream, the 1-pentyne saturator was bypassed, and hydrogen was allowed to flow over the catalyst for 1 h. The reaction was then repeated with a 1-pentyne:hydrogen ratio of 1:3. The gases evolved were analyzed as in the pulse experiments.

Hydrogenation using the same 1% $Pd/\theta\text{-}Al_2O_3$ (3.5 mg) was carried out in a closed-loop apparatus equipped with GC analysis (50-m CP-Sil glass capillary column, FID) [11]. The sample was reduced in hydrogen (400 Torr, 0.526 bar) at 358 K for 2 h before the reaction. For most of the reaction, a standard 1-pentyne pressure of 10 Torr (∼13.1 mbar) was used, and the hydrogen pressure was varied between 10 and 400 Torr (13.1–526 mbar). Other conditions at different partial pressures were also used to evaluate reaction orders. The reaction temperature was kept constant at 308 K. Catalytic experiments were realized in sequence going from higher to lower $p(H_2)$. The catalyst surface was allowed at each condition to come to steady state by repeated experiments without regeneration.

2.2. In situ TEOM experiments

The hydrogenation of 1-pentyne over $Pd/\theta\text{-}Al_2O_3$ (as above, BET surface area 97.6 $m^2\,g^{-1}$), $\theta\text{-}Al_2O_3$ (Johnson–Matthey, BET surface area 101 $m^2\,g^{-1}$), and Pd Black (Goodfellow, BET surface area 2.06 $m^2\,g^{-1}$) was studied by TEOM (Rupprecht and Patashnick, TEOM 1500 PMA) connected to an on-line gas chromatograph equipped with an FID (Hewlett–Packard 6890). The TEOM is capable of quantifying mass changes of the order of micrograms occurring in a catalyst bed during reaction, with a temporal resolution of 0.1 s. Mass changes are recorded by monitoring the change in the resonant frequency of a quartz element containing the sample in powder form packed within a small cylindrical container. The cap to the container has small holes through it such that the reactant gas stream can pass through the catalyst. During measurement, the element is made to oscillate in a clamped-free mode as a cantilever beam

by a mechanical drive [28]. As the mass of the sample increases (i.e., as molecules adsorb on to the catalyst), the frequency of the oscillation changes. Considering the system as a simple harmonic oscillator, the frequency of these oscillations is converted to a mass change through the following equation:

$$\Delta M_a = K_0\left(\frac{1}{f_1^2} - \frac{1}{f_0^2}\right), \tag{1}$$

where ΔM_a is adsorbed mass change, K_0 is spring constant, f_0 is initial frequency, and f_1 is frequency after uptake.

In particular, an increase in catalyst mass is associated with a decrease in the oscillation frequency of the TEOM. A more detailed explanation of the principles of mass measurement using TEOM has been reported by Zhu et al. [29].

For the study reported here, the catalysts (35 mg Pd/Al_2O_3, Al_2O_3, and 50 mg Pd Black) were loaded into the TEOM and constrained between 2 plugs of quartz wool (VWR). Reduction was then carried out in situ in a flow of 100% H_2 (50 $cm^3\,min^{-1}$, 1.1 bar) for 120 min at 393 K. The flow was then switched to He (50 $cm^3\,min^{-1}$, 1.1 bar), and the temperature was reduced to 358 K. Both the mass adsorbed on the three studied materials during reaction and the more tightly bound material retained after reaction were investigated as a function of exposure to 1-pentyne. 1-Pentyne was introduced to the TEOM in a carrier gas via a saturator, with the feed composition characterized by a hydrocarbon partial pressure of 0.1 bar. The carrier gas was either 100% H_2 (Pd/Al_2O_3, Al_2O_3, and Pd Black) or 5% H_2/He (Pd Black only). The pressure in the TEOM during reaction was 1.1 bar, and the temperature was 358 K. The catalyst was subjected to three periods, each 1 h long, of 1-pentyne in hydrogen. Each period was separated by 1 h of stripping with helium. The TEOM continuously recorded the mass change occurring in the sample bed, whereas GC was used to determine the product distribution at regular intervals.

2.3. In situ XPS

The in situ XPS experiments were performed at beamline U49/2-PGM1 and PGM2 at Bessy, Berlin, Germany. Details of the setup have been published earlier [30]. The photoelectron spectrometer system uses a differentially pumped lens system between the sample cell and the electron analyzer, allowing us to carry out XPS investigations during catalytic conditions in the mbar pressure range.

Four different palladium samples (5% Pd/carbon nanotubes, 3% Pd/Al_2O_3 (Johnson–Matthey), Pd(111) single crystal, and Pd foil) were introduced into the XPS cell. The 5% sample [homemade nanotubes impregnated with $Pd(NH_3)_6Cl_2$] was prepared to minimize charging effects during XPS experiments. The samples were cleaned before reaction in oxygen and then treated in hydrogen. Gas flow into the cell was controlled using mass flow controllers and leak valves. The reaction mixture consisted of 0.85 mbar H_2 and 0.05 mbar 1-pentyne. Gas-phase analysis was carried out using a quadrupole Balzers mass spectrometer connected through a leak valve to the experimental

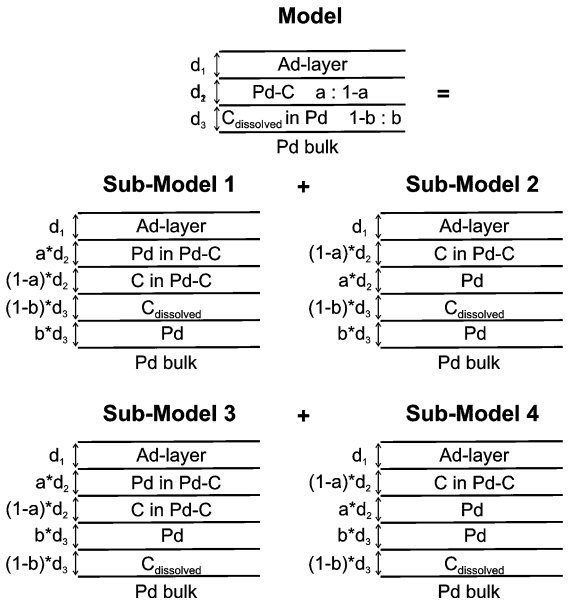

Fig. 1. Layers on plan model used to describe the experimental XPS depth distribution of carbon. "*a*" is the fraction of Pd in the Pd-C surface phase, while "*b*" is the fraction of Pd in the bulk with subsurface carbon.

cell. The geometry of the XPS cell is inadequate to realize significant conversion; therefore, conversion and selectivity values (shown in Table 3) were calculated from the product signals (after calibration), not from the decrease of 1-pentyne signal. This procedure includes a relative uncertainty of a few percentage points.

Pd3*d*, C1*s*, and valence band spectra were recorded at normal electron emission. During depth-profiling experiments, photon energies were chosen to result in photoelectrons with kinetic energies of 140, 260, 380, and 780 eV for both C1*s* and Pd3*d* core levels. Valence band was measured with 150-eV excitation. The binding energies were calibrated against the Fermi level of the samples. Pd3*d* spectra were fitted and decomposed by Gauss–Lorentz functions with an exponential tail [31]. Elemental composition was calculated after normalizing the area of measured carbon and palladium signals to their cross section [32] and to the photon flux at the applied excitation, assuming a homogeneous distribution of C in the information depth. Because the homogeneous model turned out to be incorrect, we constructed a "layers on plan" model to fit our experimental data with the following layer distribution (from the top down): adsorbate carbon, Pd-C surface phase, palladium with dissolved carbon, and carbon-free bulk palladium (Fig. 1). To facilitate calculations, the main model was subdivided into four submodels, in which the two palladium/carbon mixed layers were decomposed into four individual Pd and C layers with differing depth orders. The thickness of these new layers was defined by multiplying the atomic fraction of C (or Pd) of the actual layer with its original depth ($d2$ and $d3$). The contribution of an individual layer was calculated assuming the exponential attenuation on the above layers using the energy-dependent inelastic mean free path (IMFP) values of Pd and C from [33]. For example, the contribution of the dissolved carbon at a certain electron

kinetic energy in submodel 1 with $(1-b)d_3$ depth follows as

$$I^{C}_{(1-b)d3} = \exp(-d_1/\mathrm{IMFP_C})\exp(-ad_2/\mathrm{IMFP_{Pd}}) \times \exp\bigl(-(1-a)d_2/\mathrm{IMFP_C}\bigr) \times \bigl[1-\exp\bigl(-(1-b)d_3/\mathrm{IMFP_C}\bigr)\bigr]. \quad (2)$$

The depth of the layers and the carbon concentration of the Pd-C surface phase were allowed to vary to fit the experimental data. The carbon content of the second mixed layer ($d3$) was fixed at 0.13 atomic fraction after earlier work [24]. The total atomic fraction of carbon at a certain electron kinetic energy was calculated by summing up the carbon contribution in all of the volume compartments in all four submodels.

2.4. HRTEM

HRTEM investigation was performed in a Philips CM200 FEG electron microscope operated at 200 keV. A cross-sectional specimen was prepared from a piece of Pd foil that was previously used in the in situ XPS cell in the hydrogenation of 1-pentyne.

3. Results

3.1. Vapor-phase hydrogenation of 1-pentyne

3.1.1. Vapor-phase hydrogenation of 1-pentyne without gas-phase hydrogen

Pulses of 1-pentyne in helium were passed over 1% Pd/Al_2O_3 that had surface- and bulk-dissolved hydrogen and catalysts that had been thermally treated to desorb hydrogen. In the absence of hydrogen, the yield of pentane from the first pulse was minor (0.58%). The selectivity to pentane was 69%; 1-pentene, trans-2-pentene, and cis-2-pentene were also formed and had selectivities of 14, 14, and 3%, respectively. No gas-phase products were observed in subsequent pulses. Calculation of the amount of 1-pentyne retained by the catalyst after the first pulse gave a C:Pd(total) atomic ratio of 15:1 or a C:Pd(surface) ratio of 47. (The conversion of 1-pentyne into gas-phase products and mainly into carbonaceous deposit was 29%.) In the absence of surface- and bulk-dissolved hydrogen, adsorbed 1-pentyne must undergo self-hydrogenation to produce pentane and pentenes. Self-hydrogenation—similar to transhydrogenation [34]—can be understood as the hydrocarbonaceous deposit provides surface hydrogen to the reaction. Knowing the amount of retained 1-pentyne and the amount of hydrogen required to produce pentane and pentene, only very little (∼1%) of the hydrogen associated with the deposit is available for self-hydrogenation.

In the presence of surface hydrogen the yield of pentane was 6.73%. Over the next two pulses, the yield of pentane decreased to 1.03, then to 0.49%. A negligible amount of carbon was deposited from the first pulse, and no products were detected by the fourth pulse. However, the system in the first pulse was not selective to pentane; in contrast, 1-pentene, trans-2-pentene, and cis-2-pentene were all formed with selectivities of 70, 12, and 6%, respectively. Hence the system is selective for pentene formation on the first pulse with an overall 1-pentyne conversion of 65%. On the other hand, on pulses 2 and 3 no pentenes are formed; only pentane is formed. This is an unusual result; in keeping with literature results [15], the system would be expected move from alkane selectivity to alkene selectivity.

From the results obtained in the absence of hydrogen, it can be assumed that there is very little self-hydrogenation in the hydrogen-presaturated experiment as well (only in pulse 3); therefore, it is possible to calculate a H:Pd ratio for the hydrogen retained by the palladium and available for reaction. The calculated H:Pd(total) ratio is 13:1. This value is nonsustainable as H is dissolved in palladium; therefore, the support must play a significant role. In the absence of palladium, the support was found to be inactive; however, in the presence of palladium, hydrogen can spill over from the metal to the support. Hence there is a hydrogen reservoir, and the reverse-spillover process can supply activated hydrogen for the reaction.

The amount of carbon deposited after the third pulse (i.e., when all hydrogen has been removed) gave a C:Pd(total) ratio of 15:1, the same as that retained over the catalyst in the absence of hydrogen after the first pulse. This suggests that (surface) hydrogen can inhibit carbon deposition and that as the catalyst reaches zero or near-zero surface hydrogen concentration, the extent of retained carbon and gas-phase product yield by self-hydrogenation will be the same (pentane yield of 0.58% in the absence of H_2 and 0.49% by pulse 3 in a hydrogen-presaturated catalyst). This behavior reinforces the view that in pulse 1, not only the metal must be taken into account. If the hydrogen needed to produce the pentenes is discounted as hydrogen associated with the support, then the H:Pd ratio drops from over 13 to nearly 2, which is much more sustainable considering bulk-dissolved hydrogen and self-hydrogenation. As we discuss below, in the presence of bulk-dissolved hydrogen (and the absence of surface PdC_x; see later) the principal product of alkyne hydrogenation over palladium metal will be the alkane. Hence at higher hydrogen pressures, the catalyst will maintain selectivity to the alkane.

3.1.2. Vapor-phase hydrogenation of 1-pentyne with gas-phase hydrogen

Continuous-flow hydrogenation was carried out on the 1% Pd/Al_2O_3 as described in Section 2. Over the first 2 h, the sole gas-phase hydrogenated product was pentane. During treatment in hydrogen, 1-pentene was detected in the gas phase, confirming that the catalyst had retained C-5 species; trace levels of trans-2-pentene were also detected. The total amount of hydrocarbon removed was <1% of the feed. When the 1-pentyne feed was reintroduced at the lower hydrogen:pentyne ratio (3:1), the product profile changed such that selectivity to the alkenes was 97%. The activity was significantly lower on this run; however, a similar amount of carbon was *removed* from the catalyst in the hydrogen treatment. These results are in keeping with the proposals from the pulse reactions and the TEOM experiments (see later) at lower H:Pd ratios.

Fig. 2 shows the reaction profile obtained in the closed-loop reaction at constant 1-pentyne pressure of 10 Torr. At low hy-

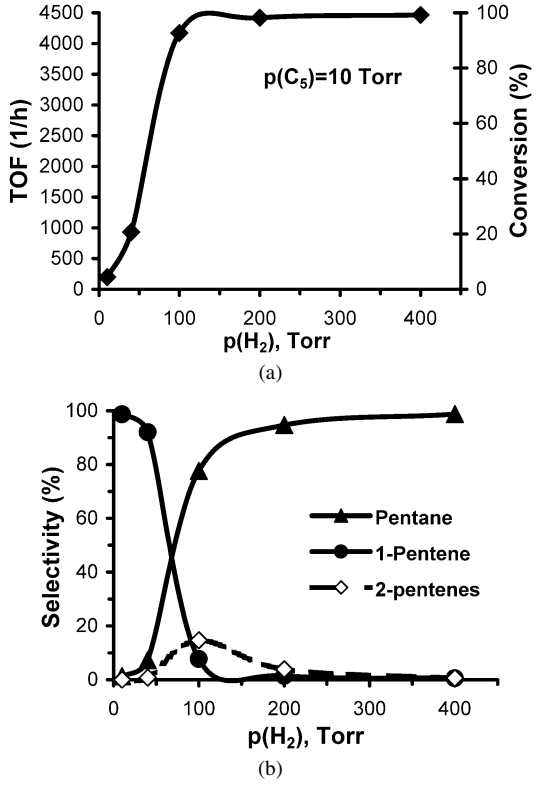

Fig. 2. 1-Pentyne hydrogenation over 1% Pd/Al_2O_3 in a closed loop-reactor, $t = 5$ min. (TOF is expressed as transformed pentyne/surface Pd atoms/time.)

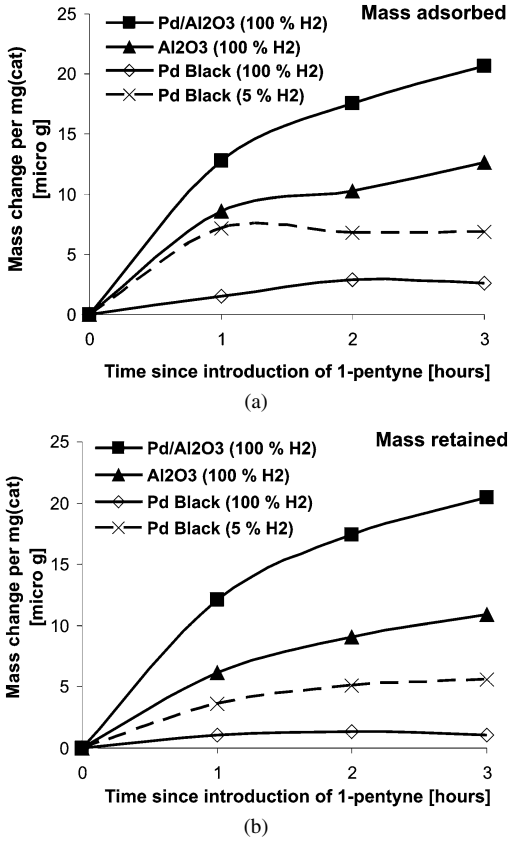

Fig. 3. (a) Mass adsorbed on catalyst after 3 × 1 h period on 1-pentyne stream. (b) Mass retained on catalyst after desorption in helium following 3 × 1 h period on 1-pentyne stream.

drogen partial pressures (low H_2-to-C_5 ratios), hydrogenation was generally selective, yielding 1-pentene. In this regime, hydrogen has a reaction order of approximately 1. At high hydrogen pressures, the activity was significantly enhanced, and nearly full conversion was observed with the selectivity pushed toward total hydrogenation. Above 100 Torr H_2, in the equilibrium regime, the hydrogen reaction order is zero and that of 1-pentyne is approximately 1. The hydrogenation rate overproportionally increased in the intermediate p(H_2) region, in which the selectivity changed drastically, indicating a transition in the reaction mechanism. This transition may correspond to the appearance of 2-pentenes in the gas phase (Fig. 2), as the surface intermediate of 1-pentene (apart from further hydrogenation) isomerizes to 2-pentenes, analogous to that shown for butenes [35].

3.2. *In situ TEOM measurements*

Fig. 3a shows the total mass change in the sample bed during each 1-h period on stream for the 4 systems studied, whereas the retained mass levels for the same systems after purging with helium are shown in Fig. 3b. The Pd/Al_2O_3 catalyst shows the greatest adsorption (per mg of catalyst) during reaction. The level of adsorption is 8 $\mu g/mg_{cat}$ greater than that on Al_2O_3 and 18.1 $\mu g/mg_{cat}$ greater than that on Pd Black under the same reaction conditions. Considering the surface composition of the materials (∼97% of the surface of Pd/Al_2O_3 is alumina compared to 100% of the pure support) this corresponds to ∼8.4 $\mu g/mg_{cat}$ of material associated with palladium sites (assuming that the alumina shows the same adsorption behavior with and without metal present). The precise composition of the adsorbed material is unknown; however, it must lie somewhere between that of pentane (the fully hydrogenated product) and elemental carbon. This provides upper and lower limits on the amount of carbon associated with each surface Pd atom of between 20.0 and 24.0 carbons per Pd. If the carbon is instead associated with the bulk Pd, then this ratio changes to 6.2–7.5 C/Pd. The effect of adsorbed hydrogen on the retained masses will be negligible even considering a β-hydride palladium phase with ∼0.7–1 H-to-Pd stoichiometry. The calculated carbon uptake number per Pd atom is extremely high; therefore, it is more likely that more carbon is adsorbed on the alumina if Pd is present. Accumulation of carbonaceous deposits on both catalytically active and inactive supports is well known in the case of reforming catalysts [36]; the amount of accumulated carbon can be 3–10 times higher on alumina than on the metallic phase if both are present; on the other hand, the amount of carbon is negligible on the support alone. The amount of retained mass (Fig. 3b) is very close to that adsorbed during reaction; hence only little desorption occurs when the catalyst is purged in He. This observation is in line with the continuous-flow experiments in which there is evidence for removal of only a minor fraction of adsorbed species.

A similar analysis provides the number of carbon atoms associated with palladium atoms on Pd Black. The BET surface area, established by nitrogen adsorption, of Pd Black is

2.06 $m^2\,g^{-1}$. The number of surface sites available for adsorption can then be calculated as follows:

$$N_{\text{sites}} = \frac{SA}{1.62 \times 10^{-19}},$$

where 1.62×10^{-19} = area of 1 molecule of nitrogen (m^2). This gives the number of surface sites as 1.27×10^{19} (g^{-1}). The total mass adsorbed on Pd Black, in 100% H_2, is 2.59 $\mu g/mg_{cat.}$ Therefore, the number of carbon atoms associated with each surface Pd atom is 8.5–10.2, and the ratio in the bulk is 0.02:1. When 5% H_2/He is used in place of pure hydrogen, a significantly greater adsorption level is achieved over Pd Black. This adsorption level of 6.88 $\mu g/mg_{cat}$ corresponds to a C:Pd_{surf} ratio of 22.6–27.2:1 and an overall C:Pd ratio of 0.05–0.06:1. The calculated Pd:C ratios for all 3 palladium-containing systems are given in Table 1.

In addition to TEOM data, on-line GC measurements were also acquired; these are summarized in Table 2. 1-Pentyne over Pd/Al_2O_3 is always converted to pentane under the study conditions. Pd Black also shows very high selectivity toward the fully hydrogenated product when 100% H_2 is used as carrier gas. However, when 5% H_2/He is used, the selectivity shifts toward 1-pentene, with the fraction of the outlet stream comprising 1-pentene increasing with time on stream. The difference between these systems can be ascribed to the higher H_2 partial pressure in the 100% system, leading to increased surface and bulk hydrogen concentrations, which will maintain catalyst selectivity to the alkane, as discussed below.

Table 1
Total quantity of material adsorbed after 3 h pentyne hydrogenation, retained after desorption, and calculated C:Pd ratios during hydrogenation

	Mass adsorbed after 3 h ($\mu g/mg_{cat}$)	Mass retained after purging with He ($\mu g/mg_{cat}$)	C:Pd-surf	C:Pd-bulk
Pd/Al_2O_3, 100% H_2	20.7	20.5	20.0–24.0	6.2–7.5
Pd Black, 100% H_2	2.6	1.1	8.5–10.2	0.02
Pd Black, 5% H_2	6.9	5.6	22.6–27.2	0.05–0.06

On first inspection, the pure alumina support also appears to show some hydrogenation activity. However, conducting identical experiments with the reactor loaded purely with quartz wool results in near-identical product selectivity. In addition, at 303 instead of 358 K, this activity is somewhat reduced. Therefore, it can be concluded that the alumina itself is inert under the conditions used herein. Blank experiments on quartz wool in the closed-loop reactor gave similar results.

3.3. In situ XPS of 1-pentyne hydrogenation

Synchrotron-radiation based high-pressure XPS was used to explore the surface and near-surface electronic structure of palladium catalysts during 1-pentyne hydrogenation. The great advantage of using a synchrotron radiation X-ray source is the possibility to perform nondestructive depth-profiling measurements. Four different palladium samples were applied in the in situ XPS experiments: two supported catalysts and two bulk palladium materials. All of these showed catalytic activity in the hydrogenation of 1-pentyne at close to 1 mbar total pressure. With the exception of the Pd(111) single crystal, which produced only pentene, both single and total hydrogenation products were formed (Table 3). Pentane is produced more in the early stage of the experiment at lower temperatures, whereas selective hydrogenation occurred at 358 K. Unfortunately, the supported catalysts in the form of pressed pellets revealed strong diffusion hindrance at 1 mbar. It is predominantly the outer part of the pellet that is responsible for the catalytic performance. One can note that despite the similar surface area, Pd foil was about three time more active than Pd(111). Moreover, the total hydrogenation selectivity was drastically decreased with bulk palladium, whereas pentane did not even form on Pd(111). This latter is in good accordance

Table 3
Conversion and selectivities in 1-pentyne hydrogenation over various catalysts at 0.9 mbar condition and 358 K

	5% Pd/CNT	3% Pd/Al_2O_3	Pd foil	Pd(111)
Conversion (%)	10	5	2.5	<1
Selectivity pentene (%)	95	80	98	100
Selectivity pentane (%)	5	20	2	–

Table 2
Gas chromatographic data for 1-pentyne hydrogenation over various catalysts. Values are reported as a percentage of the total material detected by GC at the TEOM outlet

	40 min				170 min			
	1-pentyne	1-pentene	2-pentenes	*n*-pentane	1-pentyne	1-pentene	2-pentenes	*n*-pentane
Pd/Al_2O_3, 100% H_2	trace	trace	trace	100	trace	trace	trace	100
Pd Black, 100% H_2	0.1	trace	0.1	99.8	3.6	0.5	11.3	84.5
Pd Black, 5% H_2	58.7	40.1	trace	1.2	42.8	54.7	0.2	2.3
Al_2O_3, 100% H_2	81.1	16.2	0.7	2.0	74.9	22.4	0.7	1.9
Quartz wool, 358 K	81.6	17.1	0.2	1.1	–	–	–	–
Quartz wool, 303 K	89.2	10.6	trace	0.3	–	–	–	–

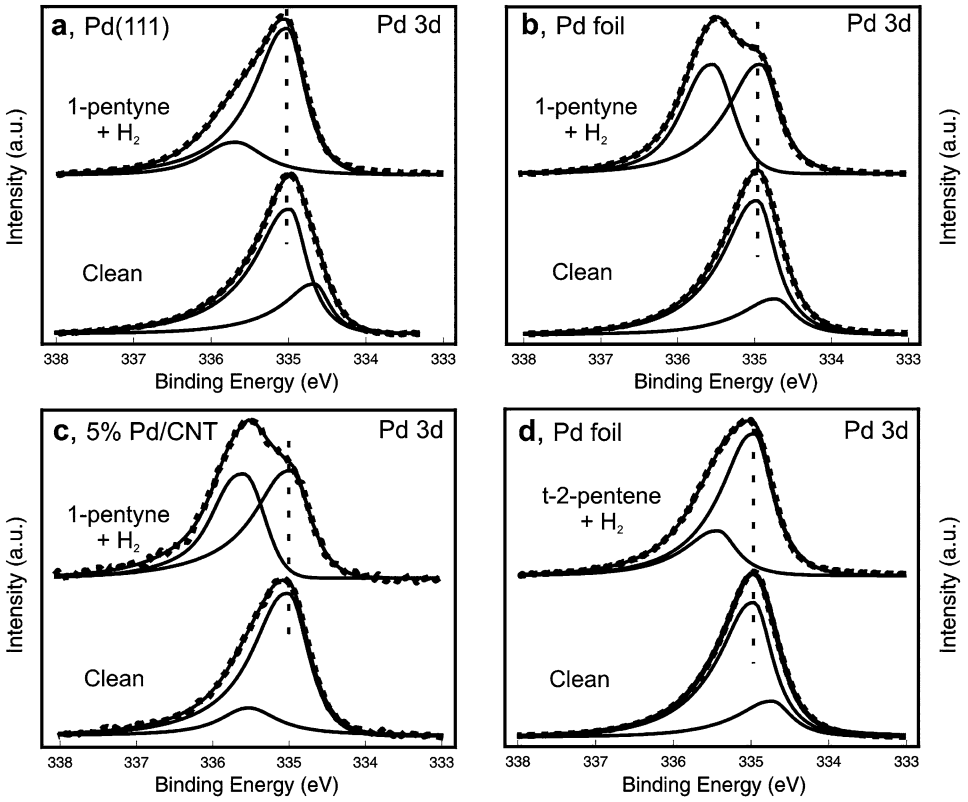

Fig. 4. Pd3*d* 5/2 of (a) Pd(111), (b) Pd foil, and (c) 5%Pd/CNT in the reaction mixture of 0.85 mbar $H_2 + 0.05$ mbar 1-pentyne at 358 K. The cleanest state of the samples is also included. As a comparison, Pd3*d* of Pd foil during the hydrogenation of trans-2-pentene (0.2 mbar *t*-2-*p* + 0.6 mbar H_2) is shown in (d). Incident photon energy, $h\nu = 720$ eV. Dashed line: measured data, full line: fits.

with our previous result [37] that pentane does not form from trans-2-pentene over Pd(111). The significantly higher total hydrogenation selectivity on the supported samples can be attributed in part to the aforementioned diffusion hindrance in the pores.

Concurrently with the mass spectrometric analysis, the surface of the samples was monitored by XPS. Fig. 4 displays the corresponding Pd3*d* (5/2) spectra at steady reaction conditions and for comparison in the state before reaction. Adsorbed (carbonaceous) species shifted the binding energy (BE) of surface palladium atoms (surface core level shift with a BE of $3d_{5/2} \sim 334.7$ eV) to the high BE side of the bulk (∼335.0 eV) palladium signal. The BE for this component was found at about 335.7 eV for Pd(111). At a very similar BE (335.6 eV) a palladium peak with significantly higher intensity was observed with the supported samples and with Pd foil. The fitting analysis revealed a peak area roughly similar to the bulk component. (Note that its apparent higher intensity was caused by the asymmetrical shape of the bulk peak.) Considering the mean free path of Pd at 720 eV (∼9 Å), this component cannot correspond to only surface Pd (see the next paragraph). In the hydrogenation of trans-2-pentene on Pd foil, this intense new component did not form (Fig. 4d); only the adsorbate-induced state formed. The asymmetry parameter of the Gauss–Lorentz function decreased considerably for the 335.6-eV component compared with the bulk component, indicating its less-metallic character. Valence-band spectra of palladium foil (Fig. 5) taken with 150-eV excitation during the steady hydrogenation point

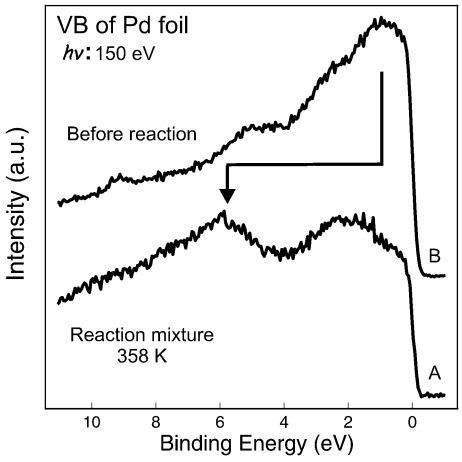

Fig. 5. Valence band of Pd foil in the reaction mixture of 0.85 mbar $H_2 + 0.05$ mbar 1-pentyne at 358 K (A) and before reaction (after cleaning, B). Incident photon energy, $h\nu = 150$ eV.

to a massive redistribution of the spectral weight in the valence band; the density of the Pd*d*-band maximum decreased while a new band at about 6 eV developed.

The synchrotron radiation X-ray source allowed us to vary the excitation energy, and hence the information depth. Obviously, depth-profiling measurements are most powerful when using microscopically planar surfaces. Fig. 6 depicts such an experiment on Pd foil in the reaction mixture. From this figure, it is obvious that the 335.6-eV component is more surface

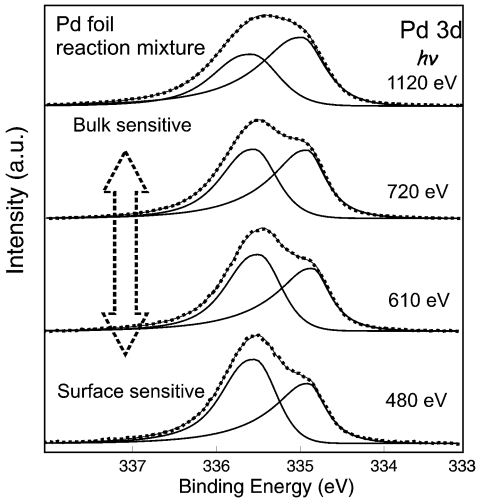

Fig. 6. Nondestructive depth profiling experiment on Pd3*d* of Pd foil during 1-pentyne hydrogenation.

located, that is, it is above the bulk Pd.

$$\text{depth}_{\text{Pd-C}} = \text{IMFP}_{\text{Pd}} \ln\left(\frac{\text{area}_{\text{Pd C}}}{\text{area}_{\text{Pd bulk}}} + 1\right). \quad (3)$$

Considering its "on-top" location and the IMFP values of Pd at different photon energies [33], the 335.6-eV component according to Eq. (3) has a 2- to 3-Pd atomic thickness. Because β-hydride formation (BE $\sim$ 335.2 eV, [38]) can be ruled out as the origin of this peak, a special Pd-C component must have formed in the reaction mixture. Therefore, in the pentyne hydrogenation at the regime of high pentene selectivity, the active surface consists not of metallic palladium, but rather of a few-atoms-thick metal–carbon surface phase formed over the course of the reaction. This spectroscopic evidence correlates perfectly with earlier studies (mentioned in the Introduction) showing that alkene formation from alkyne occurs just after the catalyst retains a significant amount of carbon on its surface. (Please note the form of Pd3*d* at 1120-eV excitation. Typical lab X-ray sources [Mg$K\alpha$, 1253.6 eV; Al$K\alpha$, 1486.6 eV] would not allow resolution of the 335.6 eV component; hence it is not surprising that such a surface Pd-C phase was not previously observed.)

As the palladium samples are heated further, their catalytic activity diminishes. Parallel to this, the 335.6 eV "Pd-C" component also strongly decreases (see later in Fig. 8), indicating its metastable nature with respect to segregation into carbon and pure palladium. In addition, at higher temperatures, most of the surface and near-surface dissolved hydrogen (α-hydride) should have desorbed or diffused to deeper layers. In the cooling experiment, after the palladium foil was heated to 523 K, neither the catalytic activity nor the 335.6-eV component recovered, strengthening their strong correlation. Once "Pd-C" decomposed, a special carbonaceous blocking layer should have formed, hindering both adsorption of hydrogen and regeneration of the active phase.

The change in the electronic structure of palladium catalyst via carbon incorporation necessarily involves the modification of its geometric structure in the near-surface layers as well. HRTEM is well suited to account for such modifications. Palladium foil used in 1-pentyne hydrogenation for the XPS experiments at low and then high temperatures indicates surface graphitic structures with few graphene layers [37]. Very rarely, up to 10–12 layers were observed. The observed inability to recover catalytic activity is therefore related to the existence of graphitic layers. Closer inspection of the palladium foil lattice fringes reveals a significant expansion of its lattice. Using Fourier transformation of selected areas of Pd lattice, the created power spectra can supply information about the depth distribution of possible lattice expansion. Table 4 summarizes the observed deviations from the ideal lattice distance calculated for several images. It is seen that lattice expansion is more pronounced in the near-surface area. The calculated standard deviation of the average lattice expansion indicates that this method is qualitative rather than quantitative for revealing this phenomenon; however, that lattice expansion exists and is more pronounced in the near-surface regions is obvious. The most feasible explanation for such lattice expansion is incorporation of carbon during the catalytic experiment.

Table 4
Average lattice expansion in Pd foil calculated for three different depths; referenced from the surface. Circles with 3 nm diameter were used for fast Fourier transformation. The lattice expansion nearest the surface was averaged from 10 calculated power spectra

Depth	Average observed deviation (%)
First 3 nm	5.4 ± 1.3
Second 3 nm	1.7 ± 1.7
Third 3 nm	3.6 ± 1.7

A very effective way of proving carbon incorporation in-situ is to perform a depth-profiling XPS experiment during a catalytic run on both palladium and carbon core levels. With the help of energy-dependent theoretical cross sections, the palladium:carbon ratio can be calculated for various information depths. Fig. 7 displays the carbon content in the reaction mixture during hydrogenation according to the depth-profiling experiment. The figure also shows simulated carbon curves using only adsorbed carbon on carbon-free bulk palladium and a more complex model described in Section 2. The simple overlayer-type model (3.5 monolayer C) cannot account for the experimental observations; thus, the presence of subsurface carbon had to be considered to fit the carbon content for greater depth of information. The best-fitting parameters describing the carbon depth profile are given in Table 5. The best fit provided an approximate 3-Å-thick layer of adsorbates on a 14-Å-thick Pd-C surface phase. While the 3 Å could account for a coverage between 0.5 and 1 monolayer considering the three-dimensionality of the adsorbate (i.e., not only one carbon atom attenuates one surface unity), the 14-Å-thick Pd-C surface phase could correspond to $\sim$3 double layers of Pd-C, that is, three alternating carbon and palladium rows. This latter would be similar to the case in which oxygen is incorporated in the ruthenium top layers, forming "trilayers" of O–Ru–O, which is thought to be the intermediate in the Ru oxidation route [39]. The calculated thickness of Pd-C fits well with that estimated from the Pd3*d* profile decomposition. The thickness

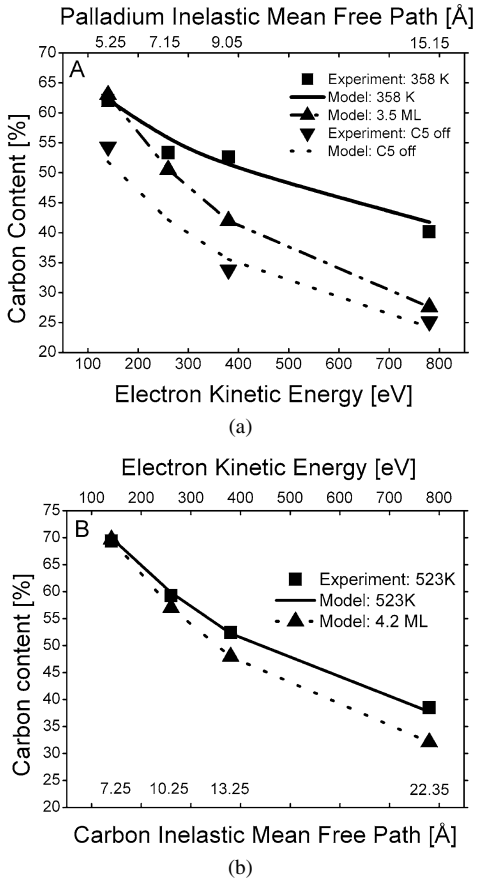

Fig. 7. Carbon distributions with different information depth as revealed by the depth profiling XPS experiments. For easy of understanding carbon content is expressed according to the homogeneous model. Calculations applying the depth model given in Fig. 1 and a simple model using only 3.5 monolayer adsorbed C (3.5 × 2.06 Å) in (a) and 4.2 ML in (b) are shown.

Table 5
Calculated parameters describing the depth profile of the palladium foil. "d_1–d_3" are the thickness of the ad-layer, that of Pd-C surface phase and of Pd bulk with dissolved carbon, while "a" is the fraction of Pd in the Pd-C surface phase and "b" is the fraction of Pd in the layer d_3, (see Fig. 1). During calculation at 358 K in the reaction mixture "b" was assumed to be 0.87 according to Ref. [24]. At 523 K, as Pd-C decomposed (see Fig. 8b) "a" was set to 1

Parameters	Reaction mixture (358 K)	Reaction mixture (523 K)	Switched off C5
$d1$	3.27	7	2.8
$d2$	14.3	3	7.4
$d3$	140	100	40
a	0.55	1	0.55
b	0.87	0.9	0.97

of the 140-Å Pd bulk with an average carbon atomic fraction of 0.13 indicates that a very significant amount of carbon is dissolved in the palladium lattice. Extrapolating the model for infinite thickness, the total amount of carbon to the surface unity (i.e., to a surface Pd atom of theoretical clean surface) would be ∼14:1, as opposed to 22-27:1 in the case of TEOM on Pd Black. Despite the different pentyne partial pressures used in the two experiments, this indicates that XPS most probably does not overestimate the carbon content of palladium.

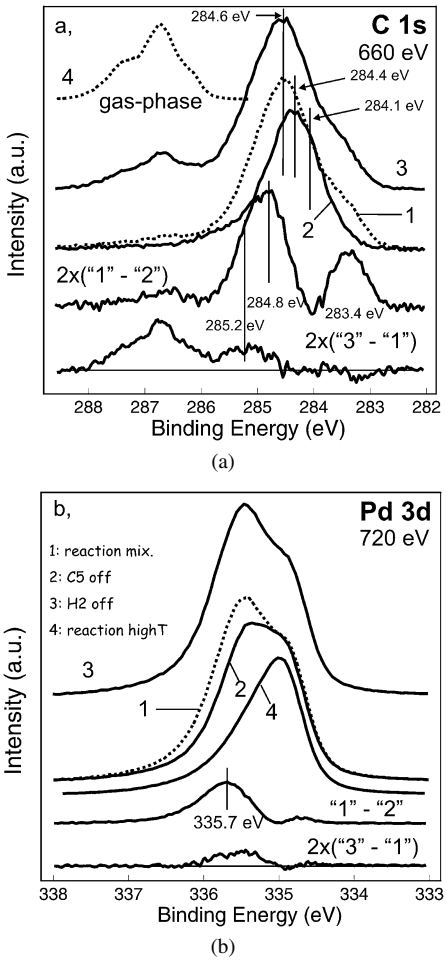

Fig. 8. (a) C1s and (b) Pd3d region of Pd foil at different conditions. 1: in the reaction mixture; 2: after switching off 1-pentyne (only H_2); 3: after switching off H_2 (only 1-pentyne). All the spectra were recorded at 358 K. Some difference spectra are also shown. In (b) Pd3d of Pd foil at 523 K is also included.

After demonstrating that the active surface of a palladium catalyst in the selective hydrogenation of pentyne consists of a Pd-C surface phase, below which a considerable amount of subsurface carbon is incorporated, we turned our attention to investigating how this system would behave when switching off one of the reactants. Fig. 8 shows the C1s and Pd3d spectra at 358 K taken in these experiments with ∼380 eV electron kinetic energy. The C1s spectrum during reaction (curve 1) reveals a maximum at 284.6 eV with a clearly visible shoulder at the low BE side (at 283.4 eV). This latter BE is close to that of carbides [40]. As 1-pentyne was switched off (curve 2), the low-BE component and a significant intensity from the high-BE side disappeared. The latter disappeared instantaneously, whereas the former took several minutes to do so. The difference in time constants of the two components suggests that these components are not directly related and are not a single species. The slight asymmetry of the peak at ∼285 eV in the difference curve (1–2) indicates that it contains two components (284.8 and 285.2 eV). Because the gas phase is not contributing to the 285-eV peak (see spectrum 4; only negligible intensity below 285.7 eV), we attribute it to chemisorbed pentyne molecules, which desorbed as the pentyne feed was stopped. After

switching back 1-pentyne, the spectrum (not shown) immediately developed as in the reaction mixture (curve 1). Moreover, a pentene signal appeared in the MS spectrum. Calculation of Pd-to-C ratios indicates a <0.5% increase of carbon content in the information depth between states before switching off and after switching back to the pentyne feed. Therefore, beam-induced carbon accumulation was not observed during this experiment. Spectrum 3 in Fig. 8 was recorded after the hydrogen supply was turned off. The signal related to 1-pentyne in the gas phase was now significantly enhanced as the scattering of the photoelectrons on the hydrogen molecules was eliminated, and thus the gas-phase signal was enhanced. Furthermore, no spectral changes indicating decomposition occurred. The difference spectrum (3–1) indicates a tiny increase at 285.2 eV, seen also as a slight broadening on the high-BE side of spectrum 3, and a very small decrease around 283.2 eV. As hydrogen was turned on, reaction continued, and again no beam-induced carbon accumulation was observed from investigation of the spectra.

The corresponding palladium 3*d* spectra to the aforementioned carbon spectra are shown in Fig. 8b. As pentyne was switched off, the "Pd-C" component partially decreased. The difference spectrum indicates a somewhat higher (335.7 eV) BE; thus, the 335.6-eV "Pd-C" component (Fig. 3) may be the sum of more than one component. In fact, carbon atoms in various environments are expected to show relaxation shifts. The original Pd3*d* spectrum was observed as pentyne was reintroduced in the feed (not shown separately). Moreover, hardly any modification was obtained with just pentyne in the feed. The slight increase at ∼335.5 might be correlated with higher pentyne coverage. In addition, the Pd3*d* spectrum in the reaction mixture at 523 K was also included, as discussed previously.

The surface state of the sample with pentyne switched off was measured with more than one excitation energy; therefore, we can estimate the palladium-to-carbon depth distribution shown also in Fig. 7a. The absence of pentyne in the gas phase reduces the total carbon content, not only on the surface. Carbon was depleted from the subsurface region; hence, the desorption of pentyne was accompanied by the migration of carbon from subsurface positions to surface positions. Because the model describing the measured carbon profile using an atomic fraction of 0.13 for dissolved carbon in palladium indicated that this layer was <15 Å thick, we allowed the carbon fraction to decrease. Hence the calculation showed a more reasonable 40-Å-thick palladium layer with only a 0.03 fraction of carbon. Generally the greatest amount of carbon was observed at 523 K in the reaction mixture (Fig. 7b), with subsurface carbon intensity less than at 358 K. However, its presence (although reduced) at high temperature is in good agreement with the HRTEM data shown previously. Moreover, the increased thickness of the ad-layer (see d_1 in Table 5) is in perfect accord with the graphene layer reportedly formed at high temperature in the hydrogenation mixture [37].

4. Discussion

In this section we extract structural information from the spectroscopic data, build a functional model of the palladium near-surface region during selective hydrogenation, and establish a relationship between carbon laydown surface orientation and selectivity. Over the last 10 years, several research teams [41–44] have provided plentiful experimental evidence revealing the important and unique chemistry of subsurface or bulk-dissolved hydrogen. Hydrogen emerging from the bulk of metal particles to the surface is significantly more energetic and thus far more reactive than surface hydrogen. However, its strength is also its weakness, at least as far as selectivity is concerned—being too active to be selective enough! Its high activity in alkene hydrogenation or in the total hydrogenation of alkynes has been clearly established [44,45]; therefore, bulk hydrogen is not the best candidate for providing good selectivity in the single hydrogenation of alkynes.

We have shown in the pulse hydrogenation experiment that surface hydrogen provided by reverse spillover from the support was very selective; however, it was used up quickly in the first 1-pentyne pulse, and no pentenes were observed in the subsequent pulses. After the accessible hydrogen was removed, carbon accumulated on the surface, and the only product observed was pentane from self-hydrogenation. Hence hydrogen released by dissociated pentyne molecules is not selective either. This is essentially a very minor process, however. Going from the pulse experiments to the real catalytic study, at high hydrogen pressure or above a certain total pressure at high H_2/C_5 ratios, hydrogenation was fast and not selective. It was not our aim to study the kinetics of total hydrogenation in depth; however, the reaction rate as $r = k[H_2]^0[\text{alkyne}]^1$ can be estimated. On the other hand, at low p(H_2) or low H_2/C_5 ratio, selectivity improves significantly while the reaction rate is significantly lowered and controlled by the surface hydrogen concentration. The estimated rate equation is $r = k[H_2]^1[\text{alkyne}]^0$, where the order of alkyne is sometimes even negative. As shown by the TEOM experiment, considerably more carbon is adsorbed and retained in this reaction regime; however, the catalyst did not exhibit long-term deactivation [19]. The activity after 170 min on stream was higher than that after 40 min on stream.

From a spectroscopy standpoint, this may be the first time that the decisive role of carbon in creating the active site for the hydrogenation of a C≡C triple bond has been evidenced. In situ XPS showed that a palladium-carbon compound was formed during hydrogenation, composed of a thin layer of ∼3Pd atomic thickness on top of metallic palladium with significant carbon incorporated in the bulk. However, the "Pd-C" layer itself seems inhomogeneous. Fig. 8 shows the removal of some carbide-like component as pentyne was switched off, but the 335.6-eV Pd-C component decreased by only ∼30%. Therefore, the carbide-like C1*s* component may correspond to one of the three Pd-C double layers in the surface phase. If we assumed that the decrease in Pd3*d* (shown by the difference curve 1–2 in Fig. 8b) corresponded to the vanishing "carbide" (the 283.4-eV component), then the calculated Pd:C ratio would be 1.88:1, that is, 35% carbon. (Note that none of these components were observed during the hydrogenation of trans-2-pentene [37]; see Fig. 4d.) To end up with a carbon content of about 45%, as suggested by the model fitting of carbon depth distribution, the other part of the "Pd-C" layer would need to be more

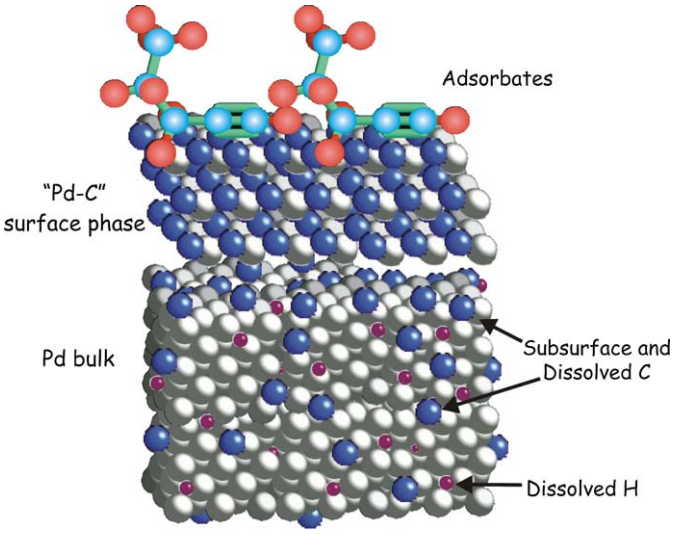

Fig. 9. Model of the palladium surface during 1-pentyne hydrogenation.

carbon-rich. The depth distribution of the Pd foil during pentyne hydrogenation is shown in Fig. 9. Pentyne was adsorbed on a C-rich "Pd-C" phase, the exact composition and geometric arrangement of which remain unknown. A thick layer with subsurface-type carbon dissolved in palladium should be the transition between the Pd-C surface phase and the bulk pure metallic palladium. The amount of carbon incorporated diminished in deeper layers. As pentyne was switched off, the adsorbed molecules desorbed, accompanied by the breakup of the less carbon-rich "Pd-C" layer and carbon segregates to the surface. As hydrogen was turned off, surface hydrogen desorbed, making space for more adsorbed pentyne, while the Pd-C double layers remained intact. At high temperature (523 K), in the reaction mixture, hydrogen and pentyne desorbed and decomposed, respectively; the double layers were destroyed; and a blocking graphene layer built up, inhibiting any further reaction. The active double layers can be restored only after regeneration, by the reaction itself.

Let us now consider the importance of the Pd-C surface phase with subsurface carbon below it. Bulk-dissolved hydrogen was shown to be reactive but unselective. As the pressure of hydrogen decreased the hydrogenation rate rapidly (overproportionally) decreased as if a preferred reaction path closed up and Pd-C was observed. It is perhaps not daring to assume that bulk hydrogen was no longer available here, because its equilibrium with the surface was disturbed by the massive amount of carbon inserted into the upper layers of palladium. Therefore, subsurface carbon and the Pd-C surface phase inhibited the repopulation of bulk-dissolved hydrogen, as well as its emergence to the surface. Whether bulk hydrogen was only "tamed down" for the reaction or was rather completely eliminated by carbon is not clear from our data. However, the usefulness of surface hydrogen in the pulse experiment points indirectly to the likelihood of the latter assumption. In fact, carburized bulk palladium showed no hysteresis in the hydrogen sorption–desorption isotherm and had no tendency toward the formation of β-hydride [46]. A very recent patent application [47] on the superiority of PdGa intermetallic compounds selectively hydrogenating acetylene in ethylene feed indicated the beneficial effects of excluding bulk-dissolved hydrogen and of isolating palladium sites on the surface.

The mechanism detailing how the Pd-C surface phase forms is not clear. Considering the carbon depth distribution, several monolayers of adsorbed pentyne are required to dissociate into C_1 species to penetrate into deeper layers and to form the top Pd-C layers. Moreover, no fragment (C_1–C_4) desorbed, because none was detected in any of the experiments. Therefore, we suspect that in the early stage, after losing the first hydrogen, the adsorbed pentyne autocatalytically fragmented and transformed into atomically dispersed carbon, which penetrated into the palladium lattice. Preliminary experiments when hydrogenating acetylene indicate that the same Pd-C surface phase was formed; hence the key point should lie in the C≡C triple bond. A supportive fact is that this surface phase did not form during the hydrogenation of trans-2-pentene when starting from a reactant with a double bond.

The last issue that we tackle here is why apparently similar palladium catalysts can behave so differently in terms of both activity and selectivity in alkyne hydrogenation [15,17,19,20], suggesting that the process is structure-sensitive. Hydrogenation was believed to be structure-insensitive, which is probably valid for ethylene hydrogenation; however, Doyle et al. [48,49] showed that pentenes react faster on larger particles, and thus the reaction exhibited structure sensitivity. Kinetic measurements on Pd(110) and Pd(111) revealed that selective hydrogenation of 1,3-butadiene was structure-sensitive as well [35]. We have seen that selectivity in pentyne hydrogenation is related to the exclusion of bulk hydrogen and thus to the buildup of Pd-C. This is possible only if the reactant strongly fragments at the initial palladium surface. Carbon–carbon bond breaking has been shown to be structure-sensitive [50,51]. Because the reaction rates when using the emerging bulk hydrogen or surface hydrogen are so different, it is not surprising that catalysts with different selectivity and hence activity can be synthesized. That different surfaces fragment differently and build up Pd-C is shown in Fig. 4, demonstrating that this process is not effective on the surface of bulk (111). In fact, DFT calculations [25] have shown that carbon diffusion into the bulk of Pd(111) is energetically unfavorable. The reason why the single crystal still performs selectively is because the applied hydrogen pressure is not sufficient to populate subsurface sites (only the α-hydride phase can form, of which hydrogen effectively penetrates to deeper layers [52,53]); therefore, only surface hydrogen was available for the reaction. However, if small palladium particles are synthesized with (111) surface plans, then they likely will be very unselective in alkyne hydrogenation, because Pd-C cannot build up and hence hydrogen can saturate the bulk of the particle, which is too reactive and not selective.

Palladium particles with the proper surface orientation or significant structural defects are required to start with the C–C dissociation reaction in the hydrogenation mixture. This will facilitate the essential carbon dissolution and buildup of a Pd-C surface phase that prevents the participation of energetic bulk-dissolved hydrogen in the hydrogenation. The competition of "Pd(C)" with "Pd(H)" is an effective concept to moderate the

availability (energy spread) of active hydrogen, thus governing the alkyne hydrogenation only toward the formation of alkenes.

5. Conclusions

In line with the literature data on alkyne hydrogenation, 1-pentyne hydrogenation on palladium catalysts was characterized by two significantly different regimes. At high pressures and high hydrogen excess, pentane is by far the main product. At lower pressures and/or lower H_2/C_5 ratios, hydrogenation is much slower, but is almost totally selective to 1-pentene. Pulse hydrogenation, in situ TEOM, in situ XPS, and HRTEM revealed that this turn of selectivity is related to carbon retention. It was unequivocally demonstrated that carbon dissolves into the palladium lattice (mainly in the near-surface region) and a palladium-carbon surface phase builds up in the early stage of the reaction. This, and not the clean palladium surface, is the active phase in the regime of selective hydrogenation of alkynes on a typical catalyst. It is proposed that the role of dissolved carbon and the Pd-C surface phase is to exclude bulk-dissolved hydrogen participating in the reaction. The genesis of the active surface includes the total fragmentation of a significant amount of reactant molecules. Furthermore, an explanation is offered for the clearly established structure sensitivity of palladium catalysts in alkyne hydrogenation. Different crystal facets will have different activities in the essential carbon laydown process. If carbon dissolution is not a favorable process [as on, e.g., the (111) facet], then the emergence of energetic bulk-dissolved hydrogen to the surface of finite-sized particles can be predicted to shift the reaction selectivity toward the formation of alkane.

Acknowledgments

Financial support was provided by the ATHENA Project and by the Humboldt Foundation through a Roman-Herzog Stipendium. The authors acknowledge the co-operation project between the Fritz-Haber Institute and the Institute of Isotopes founded by the Max-Plank Gesellschaft. The authors thank A. Klein-Hoffmann for providing the cross-sectional specimen used for HRTEM, as well as the BESSY staff for their continuing support during the XPS measurements.

References

[1] A.N.R. Bos, K.R. Westerterp, Chem. Eng. Proc. 32 (1993) 1.
[2] A.S. Al-Ammar, G. Webb, J. Chem. Soc. Faraday Trans. I 74 (1978) 657.
[3] G. Webb, Catal. Today 7 (1990) 139.
[4] N.R.M. Sassen, A.J. den Hartog, F. Jongerius, J.F.M. Aarts, V. Ponec, Faraday Discuss. Chem. Soc. 87 (1989) 311.
[5] A.J. den Hartog, M. Deng, F. Jongerius, V. Ponec, J. Mol. Catal. 60 (1990) 99.
[6] A. Borodzinski, Catal. Lett. 63 (1999) 35.
[7] D. Duca, D. Arena, A. Parmaliana, G. Deganello, Appl. Catal. A 172 (1998) 207.
[8] D. Duca, G. Barone, Zs. Varga, Catal. Lett. 72 (2001) 17.
[9] A. Sárkány, Z. Schay, G. Stefler, L. Borkó, J.W. Hightower, L. Guczi, Appl. Catal. A 124 (1995) 181.
[10] G.A. Somorjai, F. Zaera, J. Phys. Chem. 86 (1982) 3070.
[11] Z. Paál, H. Groeneweg, J. Paál-Lukács, J. Chem. Soc. Faraday Trans. 86 (1990) 3159.
[12] N.M. Rodriguez, P.E. Anderson, A. Wootsch, U. Wild, R. Schlögl, Z. Paál, J. Catal. 197 (2001) 365.
[13] M. Borasio, O.R. de la Fuente, G. Rupprechter, H.-J. Freund, J. Phys. Chem. B. Lett. 209 (2005) 17791.
[14] S.D. Jackson, N.J. Casey, J. Chem. Soc. Faraday Trans. 1 91 (1995) 3269.
[15] D.R. Kennedy, G. Webb, S.D. Jackson, D. Lennon, Appl. Catal. A 259 (2004) 109.
[16] Ph. Maetz, R. Touroude, Appl. Cat. A 149 (1997) 189.
[17] J.P. Boitiaux, J. Cosyns, S. Vasudevan, Appl. Catal. 6 (1983) 41.
[18] S.D. Jackson, G.D. McLellan, G. Webb, L. Conyers, M.B.T. Keegan, S. Mather, S. Simpson, P.B. Wells , D.A. Whan, R. Whyman, J. Catal. 162 (1996) 10.
[19] R. Marshall, G. Webb, S.D. Jackson, D. Lennon, J. Mol. Catal. A 226 (2005) 227.
[20] D. Lennon, D.R. Kennedy, G. Webb, S.D. Jackson, Stud. Surf. Sci. Catal. 126 (1999) 341.
[21] S.B. Ziemecki, G.A. Jones, D.G. Swartzfager, R.L. Harlow, J. Faber Jr., J. Am. Chem. Soc. 107 (1985) 4547.
[22] J. Stachurski, A. Frackiewicz, J. Less-Common Metals 108 (1985) 249.
[23] S.A.H. Zaidi, Appl. Catal. 30 (1987) 131.
[24] J.A. McCaulley, Phys. Rev. B. 47 (1993) 4873.
[25] L. Gracia, M. Calatayud, J. Andrés, C. Minot, M. Salmeron, Phys. Rev. B 71 (2005) 033407.
[26] M.K. Rose, A. Borg, T. Mitsui, D.F. Ogletree, M. Salmeron, J. Chem. Phys. (2001) 10927.
[27] S.D. Jackson, Sh. Shaikhutdinov, M. Heemeier, M. Bäumer, T. Lear, D. Lennon, R. Oldman, H.-J. Freund, J. Catal. 200 (2001) 330.
[28] F. Hershkowitz, P.D. Madiara, Ind. Eng. Chem. Res. 32 (1993) 2969.
[29] W. Zhu, J.M. van de Graaf, L.J.P. van den Broeke, F. Kapteijn, J.A. Moulijn, Ind. Eng. Chem. Res. 37 (1998) 1934.
[30] H. Bluhm, M. Hävecker, A. Knop-Gericke, E. Kleimenov, R. Schlögl, D. Teschner, V.I. Bukhtiyarov, D.F. Ogletree, M. Salmeron, J. Phys. Chem. B 108 (2004) 14340.
[31] D. Briggs, M.P. Seah (Eds.), Practical Surface Analysis: Volume 1—Auger and X-Ray Photoelectron Spectroscopy, Wiley, New York, 1990.
[32] J.J. Yeh, I. Lindau, Atomic Data Nuclear Data Tables 32 (1985) 1.
[33] S. Tanuma, C.J. Powell, D.R. Penn, Surf. Interface Anal. 17 (1991) 911.
[34] S.D. Jackson, I.M. Matheson, G. Webb, Appl. Catal. A 289 (2005) 16.
[35] J. Silvestre-Albero, G. Rupprechter, H.-J. Freund, J. Catal. 235 (2005) 52.
[36] J. Barbier, Appl. Catal. 23 (1986) 225.
[37] D. Teschner, A. Pestryakov, E. Kleimenov, M. Hävecker, H. Bluhm, H. Sauer, A. Knop-Gericke, R. Schlögl, J. Catal. 230 (2005) 195.
[38] D. Teschner, A. Pestryakov, E. Kleimenov, M. Hävecker, H. Bluhm, H. Sauer, A. Knop-Gericke, R. Schlögl, J. Catal. 230 (2005) 186.
[39] K. Reuter, M.V. Ganduglia-Pirovano, C. Stampfl, M. Scheffler, Phys. Rev. B 65 (2002) 165403.
[40] J. Chastain (Ed.), Handbook of X-Ray Photoelectron Spectroscopy, Perkin–Elmer, 1992.
[41] S.P. Daley, A.L. Utz, T.R. Trautman, S.T. Ceyer, J. Am. Chem. Soc. 116 (1994) 6001.
[42] S.T. Ceyer, Acc. Chem. Res. 34 (2001) 737.
[43] G. Rupprechter, G.A. Somorjai, Catal. Lett. 48 (1997) 17.
[44] A.M. Doyle, Sh. Shaikhutdinov, S.D. Jackson, H.-J. Freund, Ang. Chem. 42 (2003) 5240.
[45] K.L. Haug, T. Burgi, T.R. Trautman, S.T. Ceyer, J. Am. Chem. Soc. 120 (1998) 8885.
[46] J. Stauchurski, J. Chem. Soc. Faraday. Trans. 1. 81 (1985) 2813.
[47] J. Osswald, K. Kovnir, M. Armbrüster, R. Giedigkeit, R.E. Jentoft, T. Ressler, Y. Grin, R. Schlögl, EU patent 06005310.5 (2006), submitted for publication.
[48] A.M. Doyle, Sh. Shaikhutdinov, H.-J. Freund, Ang. Chem. 44 (2005) 629.
[49] A.M. Doyle, Sh. Shaikhutdinov, H.-J. Freund, J. Catal. 223 (2004) 444.
[50] J.A. Rodriguez, D.W. Goodman, Surf. Sci. Reports 14 (1991) 1.
[51] Z. Paál, P. Tétényi, Nature 267 (1977) 234.
[52] H. Okuyama, W. Siga, N. Takagi, M. Nishijima, T. Aruga, Surf. Sci. 401 (1998) 344.
[53] U. Muschiol, P.K. Schmidt, K. Christmann, Surf. Sci. 395 (1998) 182.